Hindawi
Indoor Air
Volume 2023, Article ID 5510449, 14 pages
https://doi.org/10.1155/2023/5510449

Research Article

Validation of In-Room UV-C-Based Air Cleaners

Xing Li[1] and Ernest R. Blatchley III[1,2]

[1]*Lyles School of Civil Engineering, Purdue University, 550 Stadium Mall Drive, West Lafayette, IN 47907, USA*
[2]*Division of Environmental & Ecological Engineering, Purdue University, 550 Stadium Mall Drive, West Lafayette, IN 47907, USA*

Correspondence should be addressed to Ernest R. Blatchley III; blatch@purdue.edu

Received 10 August 2023; Revised 7 November 2023; Accepted 14 November 2023; Published 30 November 2023

Academic Editor: Faming Wang

The risks to human health posed by airborne pathogens can be mitigated by the use of ultraviolet-C (UV-C) radiation. In general, UV-C-based systems should be applied in a manner that allows effective inactivation of airborne pathogens, while controlling human exposure to below defined limits. Among the methods used to apply UV-C radiation in indoor settings to meet these objectives are UV-C-based air cleaners. These devices can be effective for the control of airborne pathogens, but methods are needed to quantify and validate their performance. To address this need, an experiment-based method and a mathematical model were developed to quantify the effects of UV-C-based air cleaners on the concentration of an aerosolized, viral challenge agent. The method and model were demonstrated to allow quantification of disinfection efficacy and to allow translation of the results from the test environment to the application environment. The primary figure-of-merit from these tests was the clean air delivery rate (CADR), which is commonly used to characterize the disinfection efficacy of these devices. The ability of a validated air cleaner to improve indoor air quality in application settings is simulated based on the measured value of CADR from laboratory tests and the mathematical model.

1. Introduction

Coronavirus disease 2019 (COVID-19) is an infectious disease caused by severe acute respiratory syndrome coronavirus 2 (SARS-CoV-2). The primary route of transmission for SARS-CoV-2 is through aerosolized viral particles. The global COVID-19 pandemic contributed to the largest global economic crisis in more than a century [1], with substantial supply chain disruptions, loss of employment, and other issues. The pandemic disrupted nearly every aspect of life, including health care, education, commerce, tourism, and manufacturing. Attention to the COVID-19 pandemic is waning, but it is clear that this will not be the last pandemic (or even epidemic) that involves airborne, respiratory viruses [2]. As such, a prudent course of action is to develop measures that can reliably and predictably reduce the risk of transmission of airborne diseases.

UV-C irradiation has been demonstrated to be effective for the control of airborne pathogens. The structure and composition of the coronaviruses, including SARS-CoV-2, make them highly susceptible to inactivation by exposure to UV-C radiation [3–6]. More broadly, most airborne pathogens are highly susceptible to UV-C exposure [7, 8], which allows UV-C radiation to be used to effectively control the concentration of airborne pathogens and to reduce the risk of communicable disease transmission.

Implementation of UV-C-based systems for the control of airborne pathogens relies on optimization to meet two somewhat conflicting design objectives. First, the system needs to deliver sufficient UV-C radiation to accomplish effective inactivation of airborne pathogens; at present, the amount of UV-C radiation and the extent of pathogen inactivation required for a given application have not been defined by regulations or guidance. Second, the system must deliver UV-C radiation in a manner that limits human exposure to below accepted thresholds; specifically, the American Conference of Governmental Industrial Hygienists (ACGIH) has defined threshold limit values

(TLVs) for exposure of human eyes and skin as a function of wavelength [9].

There are many configurations of UV-C-based systems that can meet these objectives simultaneously. Among these are in-room, enclosed air-cleaning devices. These devices, which are the focus of the work presented herein, typically involve forced recirculation of room air through an enclosed cabinet in which one or more sources of UV-C radiation are used to irradiate air. These devices may also be configured with other forms of air treatment, such as filtration.

UV-C-based air cleaners can be used to reduce human exposure to airborne pathogens in essentially any indoor setting. Examples of settings where such devices have been used include homes, offices, retail outlets, airport terminals, and medical (clinical) settings. Reductions in pathogen exposure will translate to reductions in the risk of disease transmission. A recent market analysis suggested that the global air purifier market had a value of US $1.39 billion in 2022, with projected growth to US $4.42 billion by 2030 [10].

The ability of UV-C-based systems to reduce the risk of disease transmission was demonstrated by Wells et al. roughly 80 years ago [11, 12]; however, standards and guidance for design and implementation of UV-C-based systems for disinfection of indoor air are generally lacking. Moreover, standardized methods for testing and validation of the performance of these systems have not been developed. This lack of standardization adversely affects the application of these systems and creates opportunities for misunderstanding and misrepresentation of their behavior. Development and implementation of standardized protocols for testing and validation of these systems will improve quality control and provide transparency to users.

Kujundzic et al. [13] presented an experimental protocol to quantify the performance of in-room air cleaners, including devices that incorporated sources of UV-C radiation. Their experiments were conducted in a well-characterized indoor air quality chamber. Their tests involved the introduction of aerosolized *Mycobacterium parafortuitum* and *Aspergillus versicolor* spores to the chamber to achieve an initial concentration of the viable, airborne challenge agent; *M. parafortuitum* and *A. versicolor* spores were chosen as nonpathogenic and subpathogenic bacterial and fungal challenge agents, respectively. This was then followed by simultaneous termination of aerosol introduction and initiation of treatment. Performance of the air cleaners was quantified by following the 1st-order decay of the concentration of the challenge agent, following termination of challenge agent introduction and initiation of treatment. These tests were conducted with the air handling unit for the chamber turned off; however, an infiltration rate of 0.1-0.3 air changes per hour (ACH) was reported for their chamber. Their results indicated that the UV-C-based systems they tested provided no improvement of airborne microbial composition, relative to filtration methods. However, their results indicated that UV-C radiation was effective for inactivation of challenge agents on filter media. By comparison of the measured decay of an airborne challenge agent concentration with a model to simulate that decay, they were able to develop estimates of the microbial clean air delivery rate (mCADR) for each system. The work of Kujundzic et al. [13] provides a solid foundation for work of this type. However, the challenge agents that were applied in their work are poorly characterized in terms of their intrinsic inactivation kinetics based on exposure to UV-C radiation. It is likely that *M. parafortuitum* and *A. versicolor* spores are relatively resistant to UV-C exposure, as compared to common airborne viral pathogens, such as the coronaviruses, influenza viruses, and measles virus. Moreover, the method of following challenge agent decay offers the possibility of reaching the detection limit for the challenge agent, which will complicate interpretation of the results.

The goal of this work was to develop and apply a method to quantify the performance of in-room UV-C-based air cleaners. An experiment-based method was developed together with a corresponding mathematical model to allow quantification of a fundamental *figure-of-merit* from these tests. The model can also be used to translate results from the test environment to the application environment, thereby allowing users to make informed decisions about the implementation of such devices in indoor spaces.

2. Methods and Materials

All experiments were conducted in an indoor air quality (IAQ) chamber, housed at the Ray W. Herrick Laboratories at Purdue University. The IAQ chamber used for these experiments was a rectangular box room with floor dimensions of $4.3\,\text{m} \times 4.9\,\text{m}$ $(14' \times 16')$ and a ceiling height of $2.7\,\text{m}$ $(9')$ (room volume $\approx 57\,\text{m}^3$ or roughly $2000\,\text{ft}^3$). The IAQ chamber was equipped with a dedicated HVAC system which allowed the rate of outside air introduction to the room to be monitored in real time and controlled. The HVAC system also allowed the control and monitoring of air temperature and relative humidity. For all experiments described herein, the HVAC system for the IAQ chamber was operated at roughly 2.0 ACH, based on outside air. Air temperature was maintained between 23 and 30°C and relative humidity between 40 and 65%.

A goal for the experiments was to operate the IAQ chamber under conditions of a well-mixed air space. The well-mixed assumption implies that the timescale for an air parcel to sample the entire volume of the IAQ chamber was short relative to the time spent by the air parcel in the chamber. In practical terms, the well-mixed assumption also implies that the timescale for sampling of the entire volume of the IAQ chamber by an air parcel was short relative to the timescale for changes in the concentration of challenge agents used in the experiments. A well-mixed condition will also yield spatially uniform composition.

As an empirical measure of mixing behavior in the IAQ chamber, a series of experiments was conducted in which gas-phase CO_2 was applied as an inert tracer. For these experiments, a network of nine CO_2 monitors (Awair Omni) was positioned roughly uniformly around the IAQ chamber and approximately 1.2 m above floor level (see Figure SI-1). A tenth CO_2 monitor was used as an experimental control

and was placed outside of the IAQ chamber to monitor ambient CO_2 concentration as a function of time.

Three tracer experiments were conducted as a progression of mixing conditions. For each of these experiments, a stream of pure CO_2 was introduced from a compressed gas cylinder at a constant flow rate. CO_2 introduction started at $t = 0$ and continued for 2 hours. At $t = 2$ hours, CO_2 introduction was terminated. CO_2 concentration was monitored using the nine CO_2 monitors inside the IAQ chamber and the control CO_2 monitor for the period $0 \leq t \leq 4$ hours. For all tracer experiments and experiments involving the introduction of viral challenge agents (aerosolized phage), the HVAC system of the IAQ chamber was operated at approximately 2.0 air changes per hour (ACH).

The progression of mixing conditions was defined as follows:

(i) Experiment 1: HVAC system at 2.0 ACH

(ii) Experiment 2: HVAC system at 2.0 ACH + air flow through an air-cleaning device at the design flow rate of 1020 m^3/hr (600 cfm)

(iii) Experiment 3: HVAC system at 2.0 ACH + box fan suspended 50 cm from the ceiling operated at maximum speed

The goal of these experiments was to compare the time-course patterns of gas-phase CO_2 at the nine monitoring locations as an indication of mixing behavior within the IAQ chamber. In turn, this allowed a qualitative assessment of the operating conditions required to conform to a well-mixed behavior in the IAQ chamber. Based on these results, the box fan and the fan in the air-cleaning device were operated in all experiments that involved the introduction of challenge agents to the IAQ chamber.

The challenge agent selected for experiments involving air treatment was coliphage T1. T1 is a double-stranded DNA (ds-DNA) virus with a genome size of roughly 49 kb pairs [14]. T1 is inactivated by UV_{254} exposure at a rate that is slower than the coronaviruses and influenza viruses (see Figure SI-2). As such, the response of T1 to UV_{254} exposure is conservative, as compared to these common airborne pathogens.

2.1. Culture and Plaque Assay of T1 and Its Bacterial Host. E. coli CN-13 was used as the host bacterium. Both T1 phage and *E. coli* CN-13 were purchased from ATCC. 1.5% tryptic soy agar (TSA), 0.7% TSA ("soft" agar), and tryptic soy broth (TSB) were used as growth media. Nalidixic acid was added as an antibiotic into the growth medium. *E. coli* CN-13 were grown into the log phase with TSB at 36°C ± 1.0°C.

For propagation of T1 phage, a small amount of T1 frozen stock was added into log-phase *E. coli* CN-13 and then incubated overnight at 36°C ± 1.0°C. The resulting suspension was centrifuged $3000 \times g$ for 10 minutes. Then, the supernatant was passed through a 0.22 μm membrane filter using a syringe. The resulting mixture was mixed 50 : 50 with 40% glycerol and then frozen at -80°C as a stock viral suspension.

For quantification of T1 phage, a double agar assay was used. Base agar plates were prepared by pouring 1.5% TSA into 100 mm Petri dishes. Samples were serially diluted. A mixture of 3 mL soft agar, 0.5 mL log-phase host, and 0.5 mL serially diluted sample was poured onto the base agar plate. After overnight incubation at 36°C ± 1.0°C, circular lysis zones (plaques) were counted. The quantity of phage in a sample was expressed as plaque-forming units (pfu)/mL. Plates with 30–300 plaques were selected as countable to calculate sample concentration. A more detailed description of the method may be found in EPA method 1602 [15].

2.2. Nebulizer. A 6-jet Collison nebulizer (CH Technologies) was used to generate and introduce an aerosol suspension of T1 phage into the IAQ chamber. The liquid suspension in the nebulizer was T1 phage suspended in tryptic soy broth; the nebulizer was operated at a headspace pressure of 140 kPa (20 psi); at this headspace pressure, the nebulizer sprayed aerosols into the IAQ chamber at a liquid volumetric flow rate of approximately 24 mL/hr.

2.3. Bioaerosol Sampling. Bioaerosol samplers (SKC, Dorset, UK) were used to collect air samples from the IAQ chamber. Samples were collected by pumping air from the IAQ chamber at a constant volumetric flow rate (12.5 L/min) through a BioSampler; air flow rate through the bioaerosol samplers was maintained by the use of a vacuum pump (SKC, Dorset, UK). 20 mL phosphate buffer saline (PBS) liquid was used to trap aerosols that were pumped through the sampling device.

2.4. Air-Cleaning Device. The air-cleaning device that was the subject of these experiments was a rectangular cabinet (120 cm × 47 cm × 100 cm; $L \times W \times H$) fitted with a variable speed fan, an air filter, and a chamber for UV_{254} irradiation of air (Model M600, Roman Fountains, Inc.). Air was forced through the device at a fixed volumetric flow rate of 1020 m^3/hr (600 cfm); for one experiment, the air flow rate through the device was increased to 1530 m^3/hr (900 cfm). The device housed two low-pressure Hg lamps (nominal length = 100 cm, nominal input power = 100 W, and nominal output power = 35 W per lamp) within an area that was lined with a highly UV_{254}-reflective material. The UV lamps were centrally located within the cabinet such that human exposure to UV_{254} radiation was prevented. The configuration of the hardware described above is common for many commercially available UV-based air cleaners. As such, it is expected that the methods used to quantify the behavior of this system will translate to other devices of this type.

2.5. Challenge Agent Experiments. Figure SI-3 provides a schematic illustration of the setup of the IAQ chamber for the challenge agent experiments. Prior to initiation of each experiment, the HVAC system for the IAQ chamber was set to 2.0 ACH. Then, the T1 phage suspension was transferred to the nebulizer. Introduction of the bioaerosol suspension of T1 was initiated ($t = 0$); challenge agent introduction was maintained throughout the entire period

of each experiment (0 hours $\leq t \leq$ 4 hours). The IAQ chamber was operated with the nebulizer on with the box fan and the fan in the air-cleaning device in operation (i.e., no filtration or UV_{254} irradiation) together with the HVAC system for 2 hours. Preliminary experiments and numerical simulations (see model development below) indicated that this time was sufficient to allow the air in the IAQ chamber to converge on a steady-state condition.

Air samples were collected by continuous aspiration of air through the bioaerosol sampler for 10 mins; this process was repeated on a time interval of 15 minutes. Therefore, a total of 8 samples was collected from the IAQ chamber during the first 2 hours ($0 \leq t \leq 2$ hours) of each experiment as the system approached its first steady-state condition.

Two hours after the nebulizer was turned on, the air-cleaning device was turned on with one of the designated operating conditions. Over the following 2 hours (2 hours $< t \leq 4$ hours), air samples were collected every 15 mins, with the sample collection duration for each sample being 10 mins, as described previously. Preliminary experiments and numerical simulations indicated that this time period was sufficient to allow the air in the IAQ chamber to approach a second steady-state condition. A total of 8 samples was collected from the IAQ chamber with the air-cleaning device in operation over the period during which the treatment was activated. Figure 1 illustrates the positions of the outside air inlet, air outlet, nebulizer, bioaerosol samplers, and air-cleaning device. A total of five operating conditions were evaluated in these experiments:

(i) No filter, UV off, 1020 m^3/hr operating flow rate (control experiment)

(ii) No filter, UV on, 1020 m^3/hr operating flow rate

(iii) Filter, UV off, 1020 m^3/hr operating flow rate

(iv) Filter, UV on, 1020 m^3/hr operating flow rate

(v) Filter, UV on, 1530 m^3/hr operating flow rate

2.6. Model Description. As a guide for experimental design and for interpretation of the results of experiments, a mathematical model was developed to simulate the dynamic behavior of air quality, as defined by the infective T1 concentration, in the IAQ chamber. Figure 1 is a definition sketch for the experiments that were conducted in the IAQ chamber and for model development.

The HVAC system for the IAQ chamber was operated at a fixed target air flow rate (Q); over all experiments conducted in this project, the average of air flow rate measurements was 120 m^3/hr (corresponding to 2.1 ACH), with a standard deviation of 20 m^3/hr. For the experiments described herein, the goal was to operate the HVAC system to maintain approximately 2 ACH.

The chamber was assumed to be well mixed as a result of forced air circulation that was provided by the HVAC system, the box fan, and the fan within the air-cleaning device. The assumption of a well-mixed air space was supported by the results of CO_2 tracer experiments (see discussion above and results from tracer experiments below).

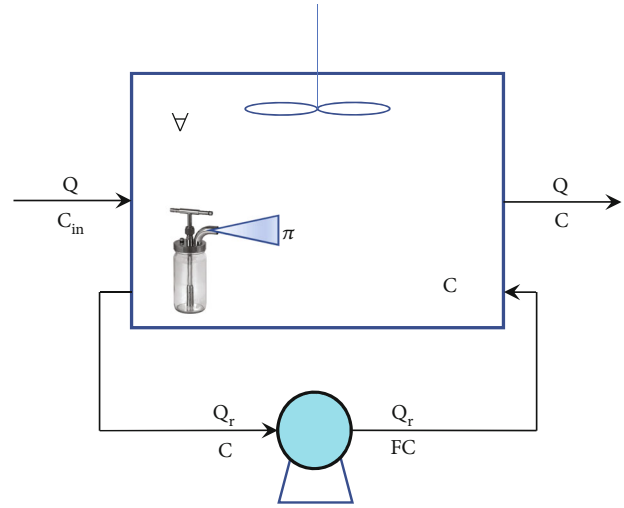

Figure 1: Schematic illustration of test setup in IAQ chamber and definition sketch for model development.

The volumetric flow rate of air through the air-cleaning device was held at one of two constant values (Q_r) for each of the experiments. The concentration of the infective, aerosolized phage in the air leaving the room through the primary exhaust vent and to the inlet of the air-cleaning device was defined as C; the same concentration was assumed at both locations due to the well-mixed condition of the room. For a given operating condition, a fixed fraction of infective phage (F) was assumed to remain in the air leaving the air-cleaning device; therefore, the concentration of infective phage leaving the device was FC. The phage introduction rate was held at a constant value (π) by maintaining constant headspace pressure in the nebulizer.

Based on the definition sketch provided in Figure 1, a material balance-based model was developed to define the time-dependent concentration of airborne infective T1 phage in the IAQ chamber during these experiments. Using the variable definitions described above, the model took the form defined in equation (1) for the period from $t = 0$ to $t = 2$ hr (i.e., period before the air-cleaning device was turned on). During this period, it was assumed that the initial infective, aerosolized phage concentration in the room was zero, as was the concentration of infective, aerosolized phage in the air entering the room from the HVAC system.

$$\forall \frac{dC}{dt} = -QC + \pi. \tag{1}$$

Dividing by ∀ and applying some algebraic rearrangement, we find

$$\frac{dC}{dt} + \text{ACH} \bullet C = \frac{\pi}{\forall}, \tag{2}$$

where ACH represents the number of air changes per hour that was accomplished by air circulation from the HVAC system. Equation (2) is a linear, ordinary differential equation

that can be solved using the "integrating factor" method. In this case, the integrating factor was defined as

$$\alpha_1 = \text{ACH}. \tag{3}$$

Applying an integrating factor of $e^{\alpha_1 t}$, equation (2) can be solved as follows:

$$Ce^{\alpha_1 t} = \frac{\pi}{\forall}\int e^{\alpha_1 t} \bullet dt + \beta_1, \tag{4}$$

where β_1 is a constant of integration that can be defined by applying an appropriate initial condition. By integration, we find

$$Ce^{\alpha_1 t} = \frac{\pi}{\alpha_1 \forall} \bullet e^{\alpha_1 t} + \beta_1. \tag{5}$$

As described above, the initial condition for this experiment was defined as $C = 0$ at $t = 0$. Substituting these conditions into equation (5), we find

$$\beta_1 = -\frac{\pi}{\alpha_1 \forall}. \tag{6}$$

Substituting this value back into equation (5), we find

$$Ce^{\alpha_1 t} = \frac{\pi}{\alpha_1 \forall} \bullet e^{\alpha_1 t} - \frac{\pi}{\alpha_1 \forall}. \tag{7}$$

Rearrangement yields an equation to define the time-dependent concentration of infective, aerosolized T1 phage for the first 2 hours of the experiment (i.e., the period before the air-cleaning device was turned on):

$$C = \frac{\pi}{\alpha_1 \forall} \bullet \left(1 - e^{\alpha_1 t}\right). \tag{8}$$

From this analysis, we can also identify the first steady-state concentration that was approached in these experiments. Specifically, if the system was allowed to operate for a long period of time, a first steady-state concentration (C_{SS_1}) would be approached:

$$C_{SS_1} = \frac{\pi}{\alpha_1 \forall}. \tag{9}$$

This first steady-state condition was assumed to represent the initial condition for the second part of the experiment, which represented the period from the time the air-cleaning device was turned on until the end of the experiment ($t \geq 2$ hr).

For this second part of the experiment, a new time variable was defined; specifically, the variable t_2 was defined to describe the time from the point at which the air-cleaning device was turned on:

$$t_2 = t - 2\,\text{hr}. \tag{10}$$

Using this new time variable and the information presented in Figure 2, it was possible to define a governing equation to define the time-dependent behavior of the infective, airborne phage in the IAQ chamber from the time at which the air-cleaning device was turned on:

$$\forall \frac{dC}{dt_2} = -QC - Q_r(C - FC) + \pi. \tag{11}$$

Following the same approach as described above, we divide both sides of this equation by $\forall$:

$$\frac{dC}{dt_2} = -\text{ACH} \bullet C - A_r C(1 - F) + \frac{\pi}{\forall}, \tag{12}$$

where $A_r = Q_r/\forall$.

Rearranging to isolate all "C" terms on the left-hand side of the equation, we find

$$\frac{dC}{dt_2} + C[\text{ACH} + A_r(1 - F)] = \frac{\pi}{\forall}. \tag{13}$$

As above, we define an integrating factor for this equation:

$$\alpha_2 = \text{ACH} + A_r(1 - F). \tag{14}$$

But we should also recognize that the clean air delivery rate (CADR) is closely related to this expression. Specifically, the formal definition of CADR is

$$\text{CADR} = Q_r(1 - F). \tag{15}$$

Substituting this expression into equation (14), we find

$$\alpha_2 = \text{ACH} + \frac{\text{CADR}}{\forall}. \tag{16}$$

This identity was important because CADR is the central *figure-of-merit* that is used to quantify the performance of air-cleaning devices. As such, it is important to be able to define its role in governing system performance as part of this model.

Substituting the definition of the integrating factor into equation (13), we find

$$\frac{dC}{\mathrm{d}t_2} + \alpha_2 C = \frac{\pi}{\forall}. \tag{17}$$

This is the same mathematical form as equation (2), and so, it will share the same general solution:

$$Ce^{\alpha_2 t_2} = \frac{\pi}{\forall}\int e^{\alpha_2 t_2} \bullet dt + \beta_2, \tag{18}$$

where β_2 is a constant of integration which we can be solved for by applying an appropriate initial condition. In this case, the initial condition is $C = C_{SS_1}$ at $t_2 = 0$.

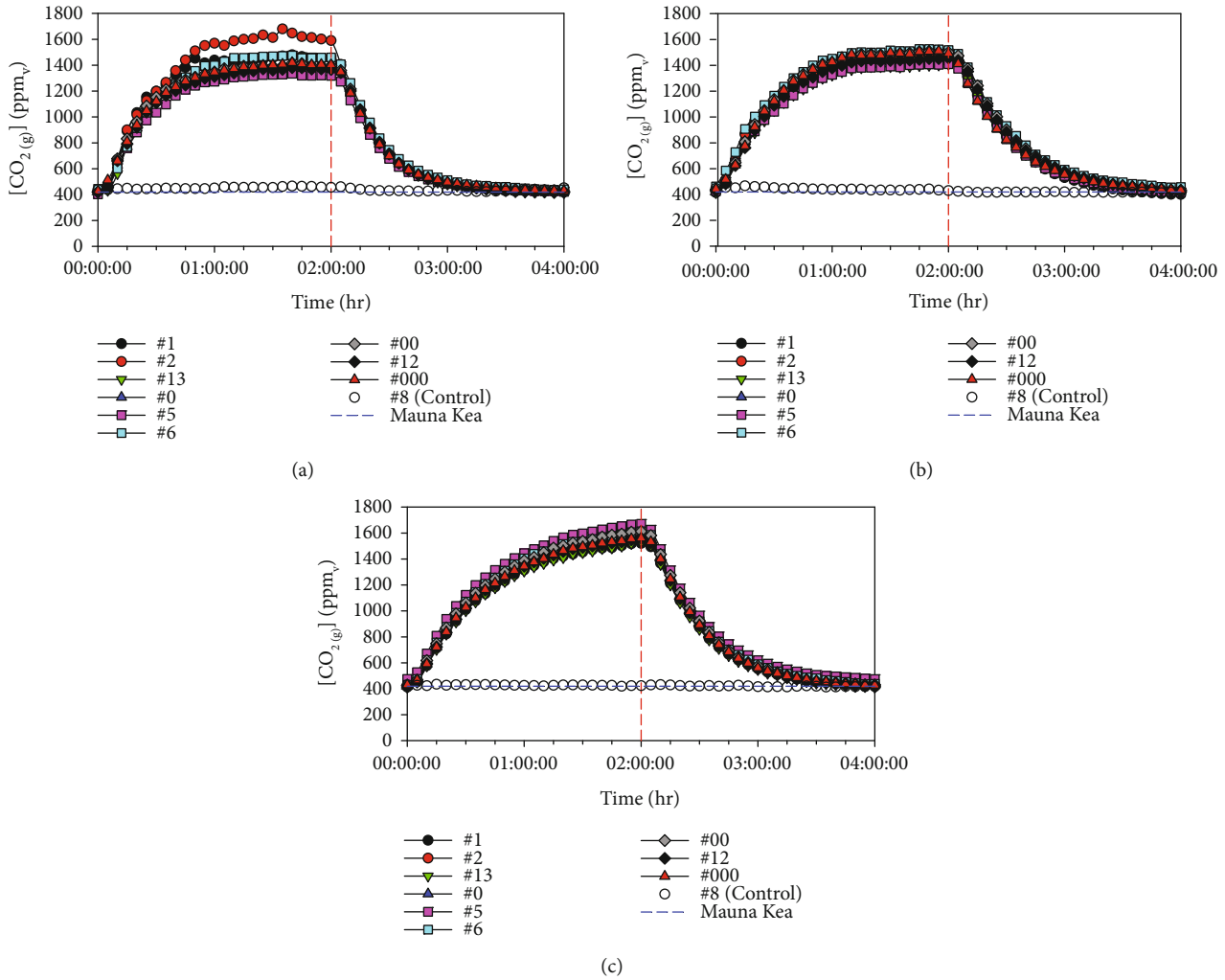

Figure 2: Results of CO_2 tracer tests. Symbols represent location-specific, time-course measurements. Vertical red-dashed line represents the time at which CO_2 introduction to the IAQ chamber was terminated. Horizontal blue-dashed line represents the average of CO_2 concentration measurements from the Mauna Kea Observatories for the period of these experiments. All experiments were conducted with the HVAC system operating at 2.0 ACH. (a) Indication of behavior with HVAC system only; (b) indication of behavior with HVAC system and air cleaner operating at 1020 m^3/hr; (c) indication of behavior with HVAC system and a box fan operating at maximum speed.

Therefore,

$$\beta_2 = \frac{\pi}{\alpha_1 \forall} - \frac{\pi}{\alpha_2 \forall}. \tag{19}$$

Substituting this identity back into equation (18), we find

$$Ce^{\alpha_2 t_2} = \frac{\pi}{\alpha_2 \forall} e^{\alpha_2 t_2} + \frac{\pi}{\alpha_1 \forall} - \frac{\pi}{\alpha_2 \forall}. \tag{20}$$

By algebra, we rearrange this equation to define an equation to describe the time-dependent concentration of the airborne, infective phage for the period starting at the time when the air-cleaning device was turned on:

$$C = \frac{\pi}{\alpha_2 \forall} + \left(\frac{\pi}{\alpha_1 \forall} - \frac{\pi}{\alpha_2 \forall}\right) \bullet e^{-\alpha_2 t_2}, \tag{21}$$

where the term $\pi/\alpha_2 \forall$ represents the second steady-state condition that the air will approach during this experiment. In other words, we can define this second steady-state condition as

$$C_{SS_2} = \frac{\pi}{\alpha_2 \forall}. \tag{22}$$

Substituting the definitions of both steady-state conditions into equation (21), we find a somewhat simpler solution to describe the time-dependent behavior of the airborne, infective phage concentration in the IAQ chamber during the second part of the experiment:

$$C = C_{SS_2} + \left(C_{SS_1} - C_{SS_2}\right) \bullet e^{-\alpha_2 t_2}. \tag{23}$$

3. Results and Discussion

3.1. CO_2 Tracer Test Results. The assumption of a well-mixed condition was important to the design of the challenge agent experiments and to the interpretation and translation of the results of those experiments. The CO_2 tracer tests were conducted with a goal of providing a qualitative understanding of mixing behavior in the IAQ chamber that resulted from air circulation by the HVAC system and the air pump within the air-cleaning device that recirculated air within the IAQ chamber. The results of the three CO_2 tracer test experiments are summarized in Figure 2.

The data from these experiments provide empirical evidence of the extent to which a well-mixed condition was met in the IAQ chamber for each of three operating conditions. For the case of the experiment in which the HVAC system was operated at 2.0 ACH and both the air cleaner fan and the box fan were turned off (Figure 2(a)), the time-course behavior of the CO_2 concentration followed a similar pattern for eight of the nine sensors; however, one of the sensors (#2) revealed a time-course CO_2 concentration that deviated substantially from the other sensors, thereby suggesting deviation from a well-mixed condition. For the case of the experiment in which the HVAC system was operated at 2.0 ACH and the air cleaner fan operated at 1020 m^3/hr (Figure 2(b)) and the box fan off, the CO_2 concentration values from the nine CO_2 sensors within the IAQ chamber approached a similar steady-state condition when CO_2 was introduced to the chamber; after CO_2 introduction was terminated, the time-course pattern of the CO_2 concentration followed a similar exponential decay pattern and returned to the baseline, ambient condition. For the case of the experiment in which the HVAC system was operated at 2.0 ACH, with the air cleaner fan turned off and with a box fan operating (Figure 2(c)), the time-course behaviors of the CO_2 concentration at all nine sensor locations were similar.

Collectively, these results suggest that a well-mixed condition was satisfactorily met when the HVAC system operated at 2.0 ACH and either the air cleaner fan operated at 1020 m^3/hr or the box fan operating. Both conditions yielded similar concentration profiles at all nine sampling locations and patterns of behavior that were consistent with the predictions of the mathematical model, which was based on a well-mixed assumption. With regard to the experiments involving T1 phage as the challenge agent, as well as the mathematical model that was developed to interpret those data, these results also supported the assumption of a well-mixed condition, which was central to the analysis of data from those experiments. In practical terms, these results also suggest that the inclusion of mechanical mixing in a room can allow an effective approach to a well-mixed condition; however, the approach to a well-mixed condition in any room will depend on room geometry, the location of mechanical mixing devices, and the amount of energy used to mix room air.

3.2. Challenge Agent Experiments. The results of measurements of airborne, infective T1 concentration from the experiments that were conducted in the IAQ chamber are summarized in Figure 3. For each experiment, the concentration of airborne, infective T1 increased rapidly for the first hour. For the period $t = 60 - 120$ minutes, the airborne, infective T1 concentration changed less rapidly, approaching a steady-state condition by approximately $t = 120$ minutes. For experiments in which UV was turned on at $t = 120$ minutes, the airborne, infective T1 concentration decreased rapidly for the first 30 minutes and then decreased more slowly to approach a second steady-state condition. For the experiment in which the filter was used without UV, the airborne, infective T1 concentration decreased less substantially than when UV was applied, the concentration approached a second steady-state condition more slowly than in the experiments that involved UV, and the steady-state airborne, infective T1 concentration was higher than when UV was applied. For the experiment that was conducted without UV and without filtration, the airborne, infective T1 concentration remained close to a steady-state condition after $t = 120$ minutes; this data set served as a control and to illustrate the stability of the steady-state condition in the IAQ chamber and as a benchmark to compare treatment results against.

The treatment condition "filter + UV, Q_1" achieved a roughly 1.0 $\log_{10}$ unit of continuous reduction of the airborne, infective T1 concentration, which was similar to "UV only, Q_1" results. The treatment condition "filter only, Q_1" resulted in a roughly 0.5 $\log_{10}$ unit of reduction of T1. The treatment condition "filter + UV, Q_2" achieved a roughly 1.2 $\log_{10}$ unit reduction of the airborne, infective T1 concentration.

It is also important to emphasize that the changes in airborne, infective T1 concentrations reported herein were based on experiments in which the challenge agent (T1) was introduced continuously. This approach was applied to facilitate quantification of the CADR (see below).

4. Regression Analysis (Least-Squares Fitting) for Estimation of System Parameters

Regression analysis (model fitting) was applied to the data from the IAQ chamber experiments with aerosolized T1 to develop estimates of the CADR for the air cleaner for each operating condition. All parameters in the model that was developed to predict the dynamic behavior of the airborne, infective T1 concentration were measured directly or could be estimated from primary measurements, except the value of α_2; methods used to estimate model parameters were as follows:

(i) The virus emission rate from the nebulizer was calculated as the product of the concentration of infective T1 in the nebulizer fluid and the volumetric flow rate of nebulizer liquid sprayed from the nebulizer (24 mL/hr)

(ii) The average of the measured airborne, infective T1 concentration measurements conducted at 80, 95, and 110 min (i.e., the last three measurements prior

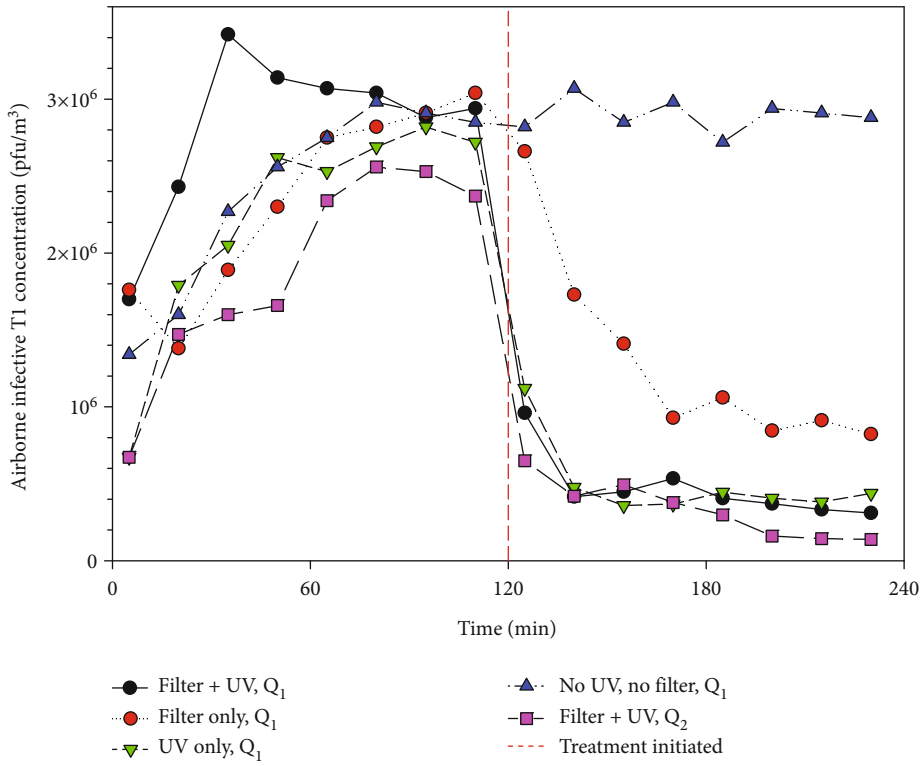

FIGURE 3: Summary of airborne, infective T1 phage concentration vs. time for five operating conditions of the air cleaner. For each experiment, $t = 0$ represents the time at which introduction of aerosolized T1 was initiated; $t = 120$ minutes represents the time at which the air cleaner was turned on (i.e., when air treatment was initiated), with operating conditions as indicated in the legend. Four of the five experiments were conducted at the air flow rate (Q_1) that represented the design condition, 1020 m^3/hr; one of the experiments was conducted at a higher air flow rate (Q_2) of 1530 m^3/hr.

to initiation of air treatment) was used as an estimate of the first steady-state concentration (C_{SS_1}, see equation (9))

(iii) The value of α_1 (ACH, see equation (3)) was calculated from the measured outdoor air flow rate into the IAQ chamber and the IAQ chamber volume

The value of α_2 was then varied as a fitting parameter. The "best-fit" value of α_2 was identified as the value that minimized the residual sum of squared errors (RSS) between the model and the measured values for the time range $0 \leq t_2 \leq 120$ minutes. Rearrangement of equation (16) allowed estimation of the CADR for each operating condition. CADR was the fundamental *figure-of-merit* to emerge from these tests.

Figures 4–7 illustrate the time-course measurements, model fits, and graphical illustrations of the approach to a minimum value of RSS for each experiment. Table 1 provides a summary of the parameter estimates for each experiment, based on model fitting to the data. Note that the effects of filtration and UV-based inactivation appear to be additive, in terms of CADR. Specifically, the sum of the CADR values for separate treatments by UV and filtration is 863 m^3/hr, whereas the value of CADR calculated for both treatments operating simultaneously was 846 m^3/hr. The sum of CADR values for filtration alone and UV alone is roughly 2% larger than the CADR value that was estimated for the combined use of filtration and UV. This is well within the error that is inherent in the measurements of the airborne, infective T1 concentration.

The error in these measurements is perhaps most clearly indicated for the experiment in which no filtration and no UV were applied (see Figure 2), especially after the system had reached a steady-state condition (i.e., after $t = 120$ min). Among these measurements, the mean was 2.90×10^6 pfu/m^3, the standard deviation was 9.99×10^5 pfu/m^3 (relative standard deviation of 3.5%), and the range was 2.72×10^6 pfu/m^3-3.07×10^6 pfu/m^3.

It is important to note that the values of CADR and F determined from these experiments depend on the challenge agent used in the tests, in this case T1. The results based on T1 are conservative, relative to coronaviruses and the influenza A virus. As such, these results can be used to indicate the lower limit of air cleaner performance for these common airborne pathogens. In other words, the results described herein represent the minimum performance that can be expected with respect to the coronaviruses and influenza A virus. With respect to these airborne pathogens, actual performance will be better than indicated by the T1 results; however, it is not possible to define, in quantitative terms, how much the performance of the air cleaner will be improved toward these airborne pathogens beyond the behavior observed with T1 as the challenge agent.

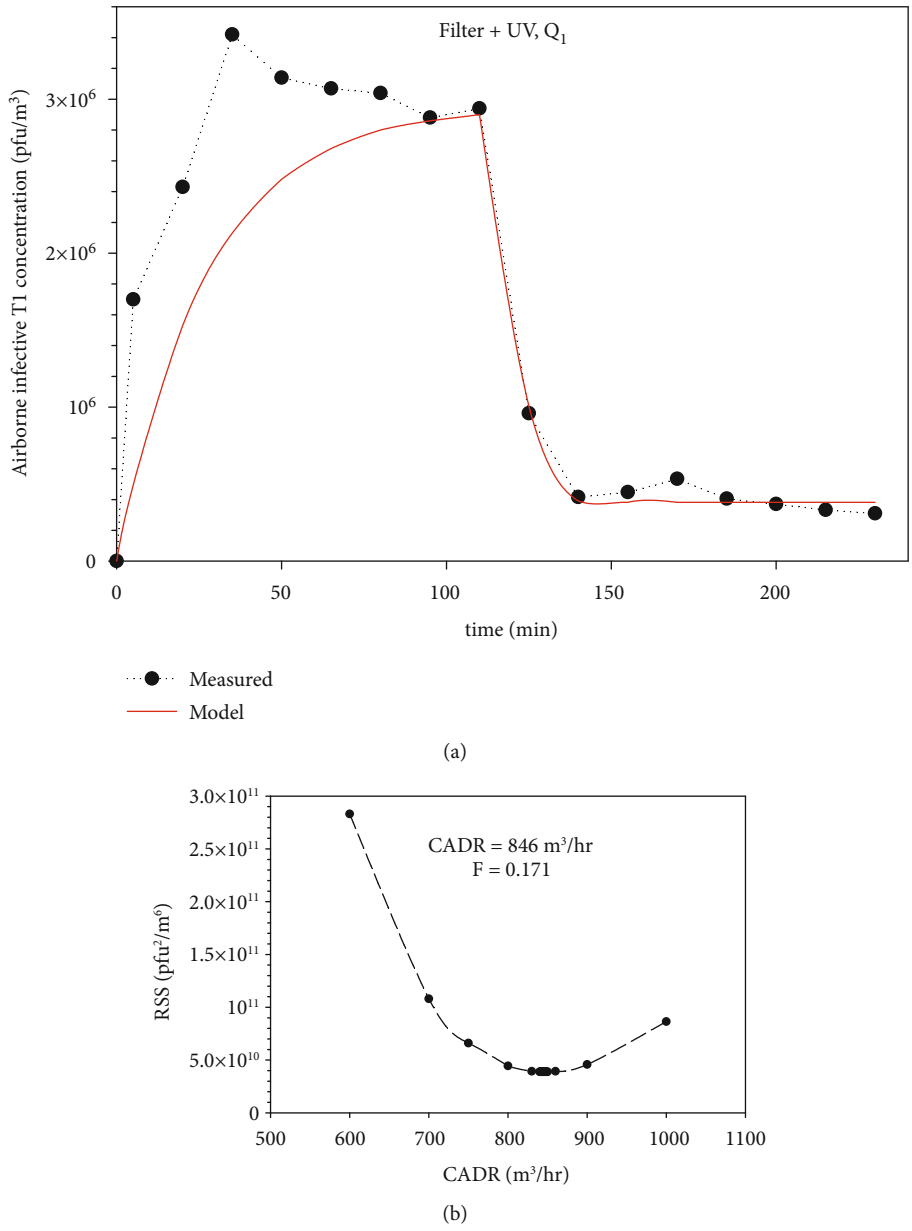

Figure 4: (a) Indication of time-course measurements of airborne, infective T1 phage concentration in the IAQ chamber for the air cleaner operated at a nominal air flow rate of 1020 m^3/hr (600 cfm) with the filter and the UV lamps both operating. Also included is a fit of the IAQ model to the data. (b) Illustration of the results of least-squares fitting of the model to the data for $0 \le t_2 \le 120$ min. The value of CADR for each experiment was identified as the value that provided the "best fit" of the model to the data, based on the minimum value of the residual sum of squared errors (RSS). The value of F for each experiment was then defined by application of a rearranged form of equation (15).

Given the values of CADR (and F) from the regression analysis, it is then possible to predict the effect of the air cleaner on air quality in a room of any size or for any pathogen emission scenario, as long as the well-mixed assumption holds. Predictions of the model for rooms of various sizes are illustrated in Figure 8. These predictions were based on a fixed value of the infective virus emission rate ($\pi = 10^5$ viruses/hr) and an assumption of a single infected individual (viral emitter) in the room. This assumed that the virus emission rate is consistent with estimates provided in several recent studies of the emission rate for SARS-CoV-2 [16–18]; however, it should be noted that reported estimates of virus emission rates vary by several orders of magnitude and appear to depend on the disease state of the infected individual, the nature of their activity, and other factors [19]. In addition, this simulation was based on an assumption of virus susceptibility to UV_{254} irradiation being similar to that of T1. As noted previously, T1 is less sensitive to UV_{254} exposure than the coronaviruses, influenza viruses, and many other common airborne pathogens; therefore, predictions of system behavior based on T1 are conservative with respect to behavior that is expected for most airborne, viral pathogens.

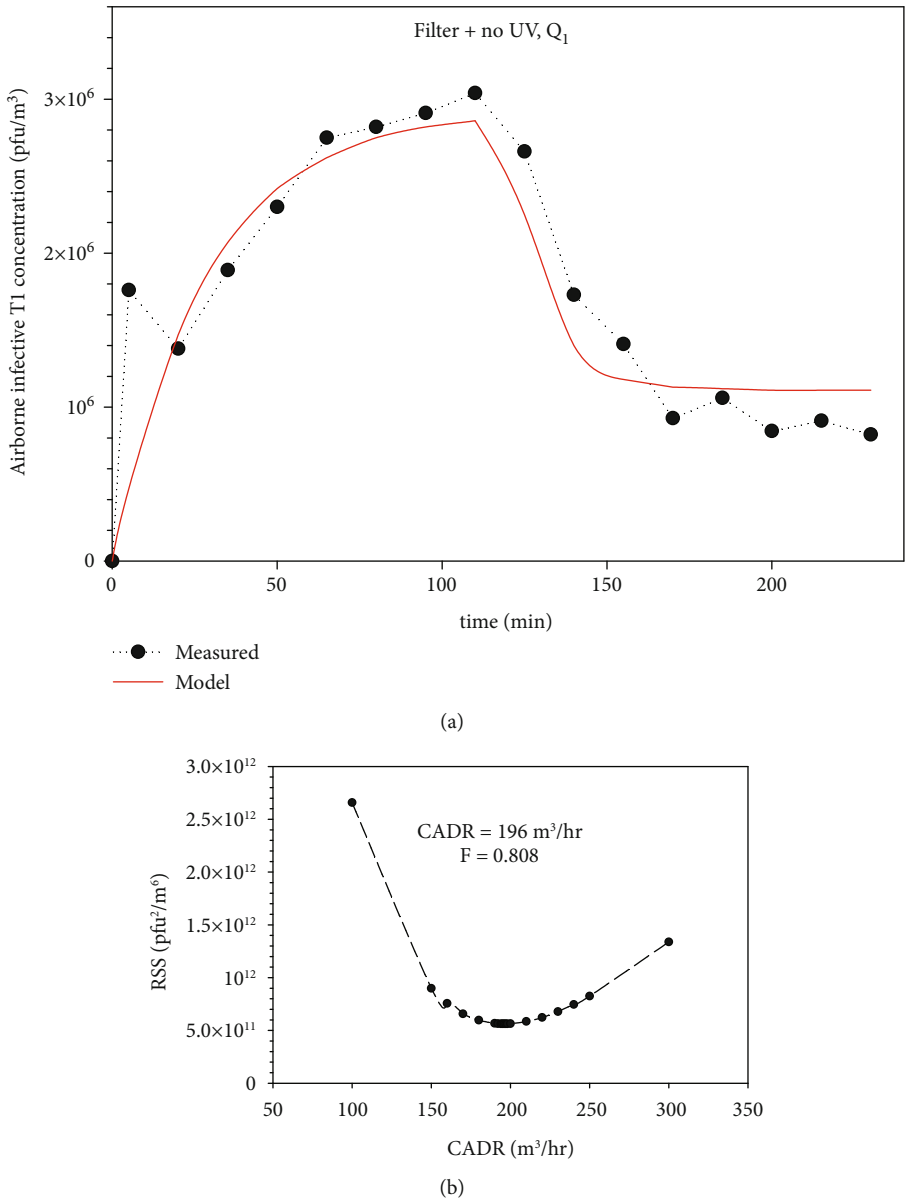

FIGURE 5: (a) Indication of time-course measurements of airborne, infective T1 phage concentration in the IAQ chamber for the air cleaner operated at a nominal air flow rate of 1020 m^3/hr (600 cfm) with only the filter operating. Also included is a fit of the IAQ model to the data. (b) Illustration of the results of least-squares fitting of the model to the data for $0 \le t_2 \le 120$ min. The value of CADR for each experiment was identified as the value that provided the "best fit" of the model to the data, based on the minimum value of the residual sum of squared errors (RSS). The value of F for each experiment was then defined by application of a rearranged form of equation (15).

The simulation was also based on an assumption of the HVAC system being operated at 1.0 ACH for all rooms. To illustrate the effects of the emitter and the air treatment system on air quality, the emitter was assumed to be present in the room for the period $0 \le t \le 4$ hr, and air treatment was assumed to be active for the period $t \ge 2$ hr. The simulations were applied for room volumes of 50 m^3, 500 m^3, and 5000 m^3; these room sizes were chosen to be representative of a range of room sizes that might be found on a university campus (dormitory room, classroom, and large lecture hall, respectively).

As indicated by the model equations, these simulations indicate that the steady-state concentration of the infective pathogen is inversely proportional to the room size; therefore, for the case of a single pathogen emitter in a room, relatively large rooms yield relatively low pathogen exposures. However, the dynamic response of the infective, airborne pathogen concentration to treatment is also influenced by room volume. As indicated in Figure 8, as room size increases, the rate at which the infective, airborne pathogen concentration changes in response to pathogen introduction or the initiation of air treatment will decrease. In all cases, the use of air treatment for the conditions described in these simulations allowed air quality to recover to a condition of essentially no infective, airborne pathogens after within 1-2 hours of the departure of the pathogen source (i.e., the

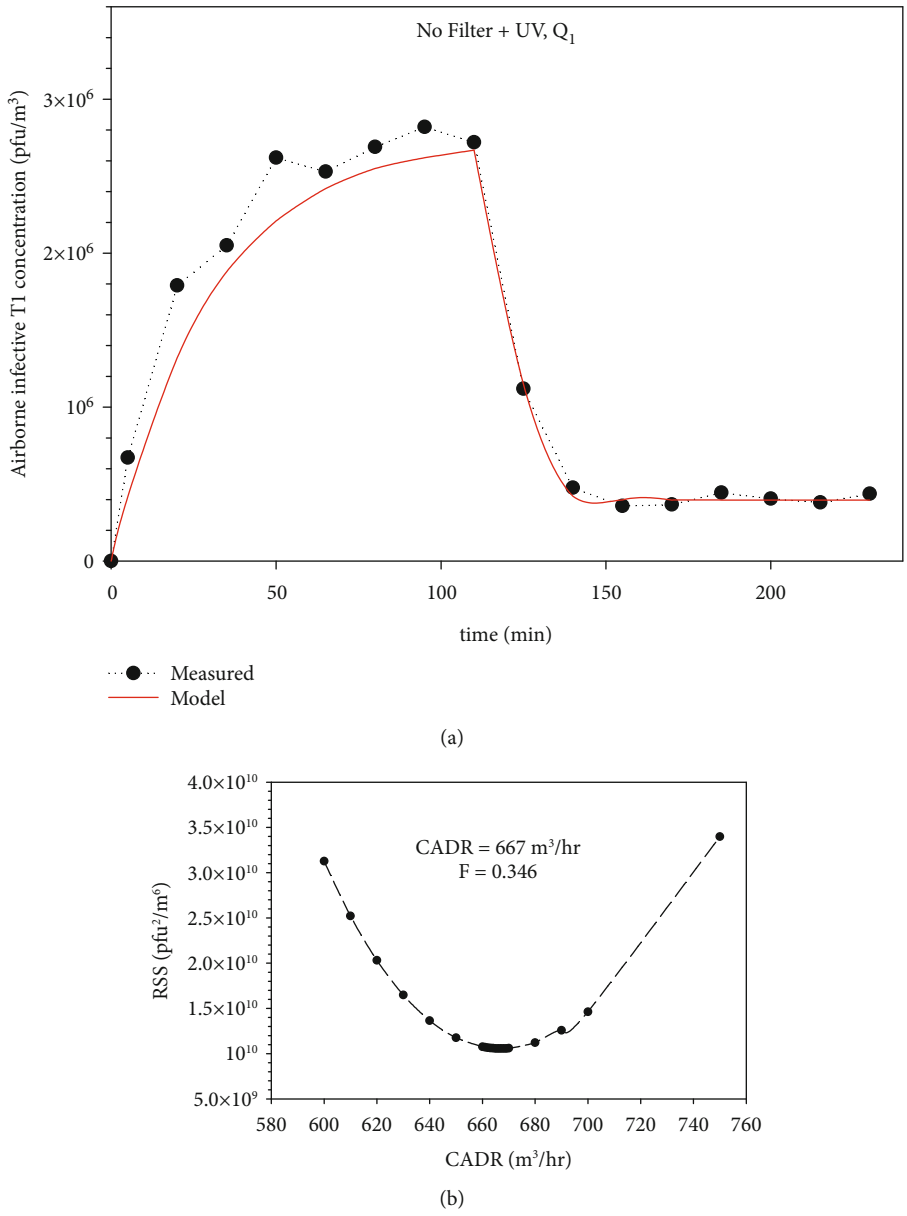

Figure 6: (a) Indication of time-course measurements of airborne, infective T1 phage concentration in the IAQ chamber for the air cleaner operated at a nominal air flow rate of 1020 m^3/hr (600 cfm) with only the UV lamps operating. Also included is a fit of the IAQ model to the data. (b) Illustration of the results of least-squares fitting of the model to the data for $0 \le t_2 \le 120$ min. The value of CADR for each experiment was identified as the value that provided the "best fit" of the model to the data, based on the minimum value of the residual sum of squared errors (RSS). The value of F for each experiment was then defined by application of a rearranged form of equation (15).

emitter) from the room; the rate of loss of infective, airborne pathogens under these conditions was inversely proportional to the room volume.

The results presented in Figure 8 illustrate the translation of results of the system testing from the test environment to the application environment. The ability to translate results from the test environment to an application environment is critical to any validation method, and it depends on the use of a test method and model that are consistent with the relevant physics. Validation methods that lack this ability are of limited value.

The tests described herein were based on the use of a single challenge agent: coliphage T1. While use of T1 is justified based on its conservative response to UV_{254} radiation, as compared to common airborne pathogens like the coronaviruses and influenzas viruses, there are some airborne pathogens that are more resistant to UV-C exposure than T1, including some bacterial spores and fungi. Moreover, the use of a challenge agent that behaves more like the coronaviruses and influenza viruses will provide a more accurate indication of the ability of a UV-C-based air cleaner to inactivate these pathogens. Similarly, the emergence of alternative sources of UV-C radiation, such as UV LEDs and excimer lamps, allows for the development of air cleaners that rely on other wavelengths in the UV-C range. For these devices, it will be important to select a challenge agent that

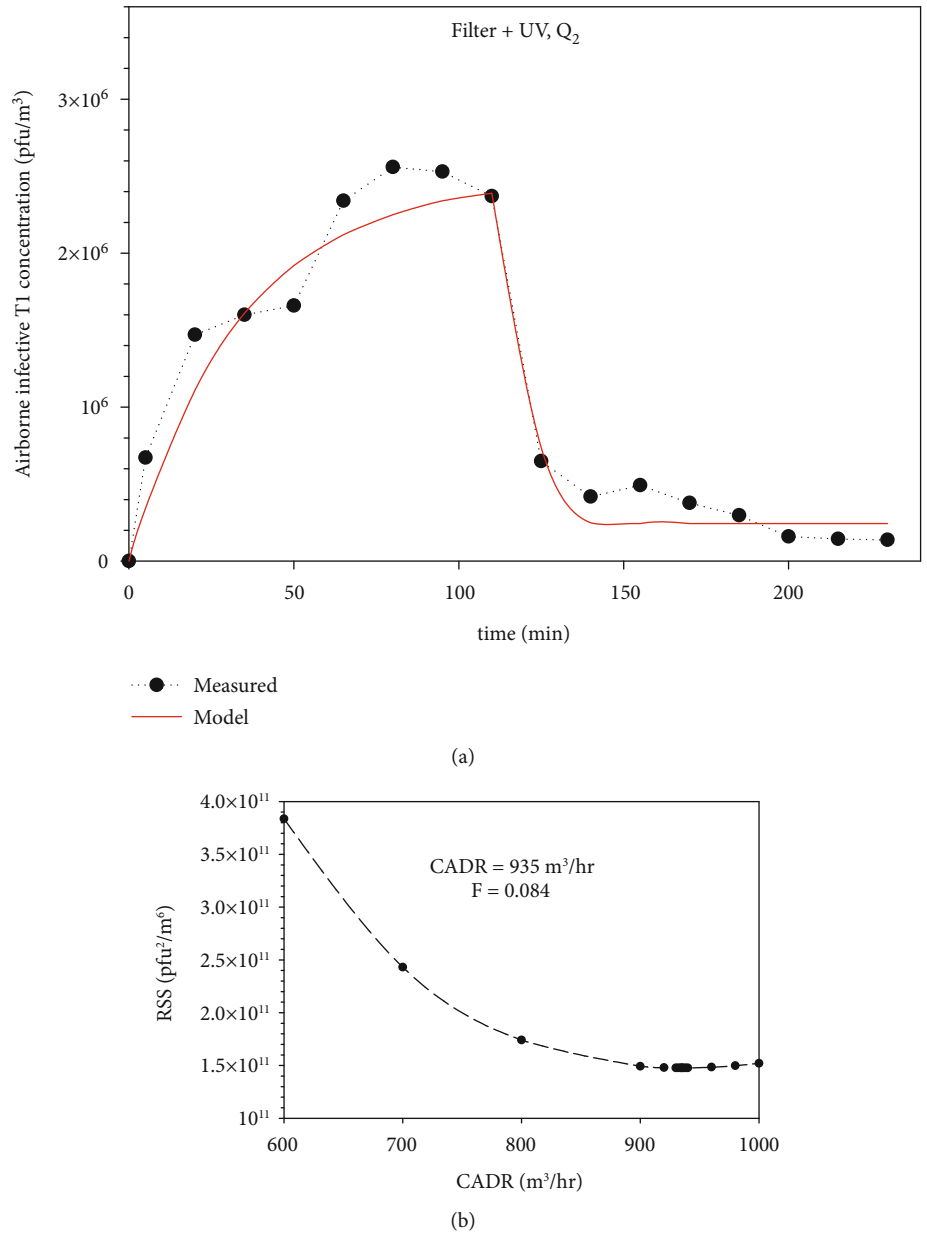

Figure 7: (a) Indication of time-course measurements of airborne, infective T1 phage concentration in the IAQ chamber for the air cleaner operated at a nominal air flow rate of 1530 m^3/hr (900 cfm) with the filter and the UV lamps both operating. Also included is a fit of the IAQ model to the data. (b) Illustration of the results of least-squares fitting of the model to the data for $0 \le t_2 \le 120$ min. The value of CADR for each experiment was identified as the value that provided the "best fit" of the model to the data, based on the minimum value of the residual sum of squared errors (RSS). The value of F for each experiment was then defined by application of a rearranged form of equation (15).

Table 1: Summary of estimated clean air delivery rate (CADR) and fraction of virus (phage) remaining in air after a single pass through the unit (F).

Operating condition	CADR (m^3/hr)	F
Filter + UV, Q_1	846	0.171
Filter only, Q_1	196	0.808
UV only, Q_1	667	0.346
Filter + UV, Q_2	935	0.084

provides a conservative response, relative to the relevant airborne pathogens.

The results of the experiments and modeling described herein provide information to indicate the ability of UV-C-based air cleaners to reduce the concentration of airborne pathogens. However, it is likely that risk-based treatment standards will be developed for these and other air treatment devices. To meet this objective, future work should link the results of the model simulations described herein to a risk-based model to allow for the development of design and operating standards that will link the physical characteristics

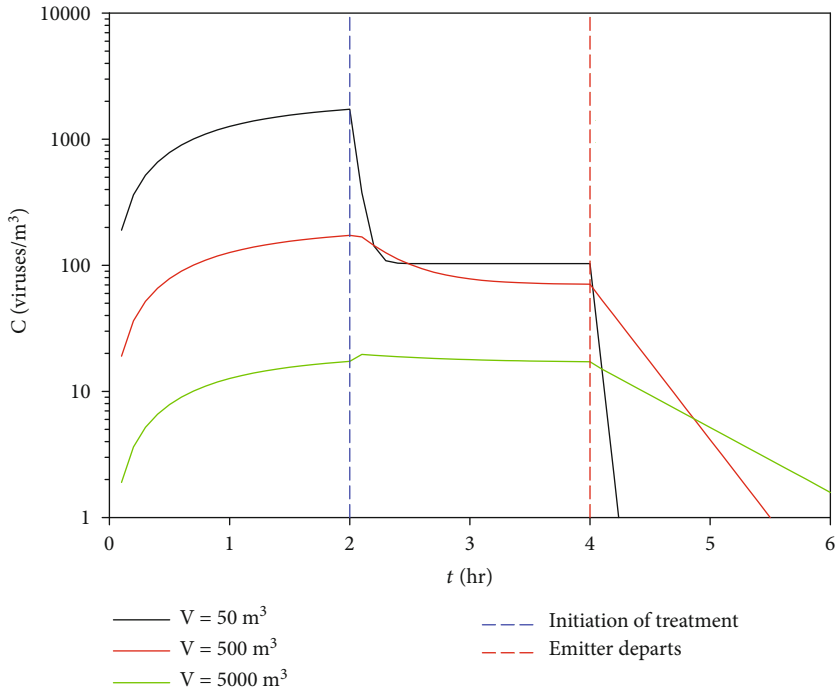

FIGURE 8: Model predictions of the concentration of infective virus ($\log_{10}$ scale) in rooms of varying size, as a function of time. Each room was assumed to be operated under conditions of 1.0 ACH and a well-mixed air space. A single emitter ($\pi = 10^5$ viruses/hr) was assumed to be present in the room for the period $0 \le t \le 4$ hr; air treatment was assumed to be initiated at $t = 2$ hr at a constant condition of $Q_r = 1020$ m^3/hr and $F = 0.10$ (CADR = 918 m^3/hr). Vertical dashed lines indicate initiation of treatment (blue) and departure of the emitter from the room (red).

of a UV-C-based air cleaner to an estimate of the disease transmission risk.

5. Conclusions

An empirical method and corresponding mathematical model are presented for use in the testing and validation of UV-C-based in-room air cleaners. Collectively, the method and model allow for the quantification of the performance of UV-C-based air cleaners and for the translation of results from the test environment to the application environment. The availability of such a test method and model allows for quantification and prediction of system performance and is critical to the design of installations based on this technology. The test protocol and model described herein were developed to describe and predict air quality dynamics in indoor air spaces in response to the implementation of UV-C-based air cleaners. These approaches can be applied for essentially any such device; these methods could be easily translated to the testing and simulation of other indoor air-cleaning devices. Moreover, these methods could be adapted to incorporate other challenge agents if a need exists to examine or predict the behavior of these systems with respect to other airborne pathogens. Similarly, these methods could be translated for examination and prediction of the behavior of UV-C-based systems that are built around alternative sources of UV-C radiation, such as UV LEDs or excimer lamps.

Data Availability

Data from the experiments and a spreadsheet-based version of the model are available upon request.

Conflicts of Interest

The authors have no conflicts of interest with respect to this work.

Acknowledgments

Funding for this project was provided by a grant from Roman Fountains, Atlanta, GA.

Supplementary Materials

Figure SI-1: schematic illustration of IAQ chamber setup for CO_2 tracer experiments. Red hexagons indicate approximate locations of the CO_2 sensors; the identifying number of each sensor is indicated within each hexagon. The air cleaner was positioned on the floor. CO_2 monitors were positioned roughly 1.2 m above floor level. The exhaust vent was located on the ceiling. When used, the box fan (not illustrated) was suspended from the ceiling, directly above CO_2 monitor #5. Figure SI-2: summary of UV_{254} dose-response behaviors for coronaviruses, influenza A virus, and coliphage T1. Red symbols indicate coronaviruses [1–4]; blue symbols indicate influenza A virus [5, 6]; green symbols indicate T1. In the case of influenza A virus, three of the data sets come from

a study in which aerosolized viruses were subjected to UV_{254} irradiation. For all other data sets, the viruses were exposed to UV_{254} irradiation while suspended in an aqueous (liquid) medium. Figure SI-3: schematic illustration of IAQ chamber setup for challenge agent experiments. The HVAC system for the IAQ chamber was operated at approximately 2.0 ACH. Air flow rate through the air cleaner was maintained at a constant flow rate of 1020 m^3/hr or 1530 m^3/hr. Aerosolized (nebulized) challenge agent (T1 phage) was introduced from a 6-jet Collison nebulizer. Aerosol samples were collected using impaction bioaerosol samplers. *(Supplementary Materials)*

References

[1] World Bank, "The Economic Impacts of the COVID-19 Crisis," 2022, https://www.worldbank.org/en/publication/wdr2022/brief/chapter-1-introduction-the-economic-impacts-of-the-covid-19-crisis.

[2] M. Marani, G. G. Katul, W. K. Pan, and A. J. Parolari, "Intensity and frequency of extreme novel epidemics," *Proceedings of the National Academy of Sciences*, vol. 118, no. 35, article e2105482118, 2021.

[3] J. L. Sagripanti and C. D. Lytle, "Estimated inactivation of coronaviruses by solar radiation with special reference to COVID-19," *Photochemistry and Photobiology*, vol. 96, no. 4, pp. 731–737, 2020.

[4] B. Pendyala, A. Patras, B. Pokharel, and D. D'Souza, "Genomic modeling as an approach to identify surrogates for use in experimental validation of SARS-CoV-2 and HuNoV inactivation by UV-C treatment," *Frontiers in Microbiology*, vol. 11, article 572331, 2020.

[5] N. C. Rockey, J. B. Henderson, K. Chin, L. Raskin, and K. R. Wigginton, "Predictive modeling of virus inactivation by UV," *Environmental Science & Technology*, vol. 55, no. 5, pp. 3322–3332, 2021.

[6] M. A. Schuit, T. C. Larason, M. L. Krause et al., "SARS-CoV-2 inactivation by ultraviolet radiation and visible light is dependent on wavelength and sample matrix," *Journal of Photochemistry and Photobiology B: Biology*, vol. 233, article 112503, 2022.

[7] W. Kowalski, *Ultraviolet Germicidal Irradiation Handbook: UVGI for Air and Surface Disinfection*, Springer-Verlag, 2009.

[8] E. R. Blatchley III, *Photochemical Reactors: Theory, Methods, and Applications of Ultraviolet Radiation*, Wiley, 2022.

[9] ACGIH, *2022 TLVs and BEIs*, American Conference of Governmental Industrial Hygienists, 2022.

[10] C. M. Insights, "UV air purifier market analysis," 2023, https://www.coherentmarketinsights.com/market-insight/uv-air-purifier-market-5643.

[11] W. F. Wells, M. W. Wells, and T. S. Wilder, "The environmental control of epidemic contagion," *American Journal of Hygiene*, vol. 35, no. 1, pp. 97–121, 1942.

[12] W. F. Wells, "Air disinfection in day schools," *American Journal of Public Health and the Nation's Health*, vol. 33, no. 12, pp. 1436–1443, 1943.

[13] E. Kujundzic, F. Matalkah, C. J. Howard, M. Hernandez, and S. L. Miller, "UV air cleaners and upper-room air ultraviolet germicidal irradiation for controlling airborne bacteria and fungal spores," *Journal of Occupational and Environmental Hygiene*, vol. 3, no. 10, pp. 536–546, 2006.

[14] M. D. Roberts, N. L. Martin, and A. M. Kropinski, "The genome and proteome of coliphage T1," *Virology*, vol. 318, no. 1, pp. 245–266, 2004.

[15] EPA, *Method 1602: male-specific (F+) and somatic coliphage in water by single agar layer (SAL) procedure*, Office of Water, Washington, D.C., 2001.

[16] J. Ma, X. Qi, H. Chen et al., "Coronavirus disease 2019 patients in earlier stages exhaled millions of severe acute respiratory syndrome coronavirus 2 per hour," *Clinical Infectious Diseases*, vol. 72, no. 10, pp. e652–e654, 2021.

[17] M. Riediker and D. H. Tsai, "Estimation of viral aerosol emissions from simulated individuals with asymptomatic to moderate coronavirus disease 2019," *Jama Network Open*, vol. 3, no. 7, article e2013807, 2020.

[18] S. L. Miller, W. W. Nazaroff, J. L. Jimenez et al., "Transmission of SARS-CoV-2 by inhalation of respiratory aerosol in the Skagit Valley Chorale superspreading event," *Indoor Air*, vol. 31, no. 2, pp. 314–323, 2021.

[19] G. Buonanno, L. Stabile, and L. Morawska, "Estimation of airborne viral emission: quanta emission rate of SARS-CoV-2 for infection risk assessment," *Environment International*, vol. 141, article 105794, 2020.